

Chimia 43 (1989) 248–256
 © Schweizerischer Chemiker-Verband; ISSN 0009-4293

In-Situ X-Ray Absorption Spectroscopic Studies of Ions at Oxide-Water Interfaces

Gordon E. Brown Jr.*, George A. Parks, and Catherine J. Chisholm-Brause

Instructive insight is gained from a novel application of synchrotron-based EXAFS spectroscopy to the study of metal complexes sorbed at oxide/water interfaces. Fluorescence-yield X-ray absorption measurements were made on high surface area, wet oxide samples with less than monolayer sorbate coverages using high intensity synchrotron radiation. The samples studied included Co^{2+} (aq) on $\gamma\text{-Al}_2\text{O}_3$ and TiO_2 (rutile), Pb^{2+} (aq) on $\gamma\text{-Al}_2\text{O}_3$, and aqueous selenate and selenite ions on $\alpha\text{-FeOOH}$ (goethite). Direct, in-situ measurements of the average distances, numbers, and identities of first- and second-neighbors surrounding the sorbed atoms in these samples were derived from the experimental data. – The results for Co^{2+} on $\gamma\text{-Al}_2\text{O}_3$ and TiO_2 , at pH 6.8, indicate that Co^{2+} forms inner-sphere complexes, that it does not sorb as a three-dimensional precipitate or diffuse into the oxide, and that it forms multi-nuclear complexes on $\gamma\text{-Al}_2\text{O}_3$ but smaller polymers or monomeric complexes on TiO_2 . – Results for Co^{2+} on $\gamma\text{-Al}_2\text{O}_3$ provide the first, direct structural evidence for multi-nuclear metal sorption complexes on an oxide surface. These results also indicate that the nature of the oxide surface influences the type of adsorption complex formed. – The sorption complexes formed by Pb^{2+} on $\gamma\text{-Al}_2\text{O}_3$ at pH 6.0 are similar; Pb^{2+} probably forms dimeric or a combination of monomeric and small multi-nuclear complexes. – Selenate is sorbed as an outer-sphere complex (pH 3.5) and selenite is sorbed as an inner-sphere, bi-dentate complex (pH 5.6) on $\alpha\text{-FeOOH}$. These structural results provide the first molecular-level explanation for the weak binding of selenate and the strong binding of selenite at the goethite/water interface.

1. Introduction

Reactions of aqueous solutes with the surfaces of solid oxides play major roles in a wide variety of contexts such as partitioning of contaminants in natural waters and in soils, dissolution/precipitation of minerals, corrosion, and electrochemical processing. Because of their importance, a great deal of effort has been devoted to characterizing such reactions; however, they remain poorly understood at the molecular level. A knowledge of surface complexes at this level is essential for quantitative thermodynamic and kinetic description of interfacial processes^[1–3].

In an effort to relate macroscopic (thermodynamic and kinetic) and microscopic (structural) information on sorption processes, a few investigators have studied them using both solution chemistry and spectroscopic methods with impressive results. The spectroscopic methods employed, however, yield largely indirect and often qualitative structural information. Furthermore, not all of these methods can be applied *in-situ*, i.e., with the sorbent still in contact with the aqueous phase. To provide more quantitative structural and compositional information about sorption complexes *in-situ*, our group has initiated a series of synchrotron-based X-ray absorption spectroscopic studies of metal ions sorbed onto wet oxide surfaces. The resulting information from this novel application of X-ray absorption spectroscopy permits more definitive discrimination among



Gordon E. Brown, Jr.: Born 1943 in San Diego, California, USA. Majored in chemistry and geology at Millsaps College, Jackson, Mississippi, where he obtained B.S. degrees in 1965. Studied crystallography, mineralogy, and inorganic chemistry at the Pennsylvania State University and the Virginia Polytechnic Institute and State University, receiving M.S. and Ph.D. degrees in 1968 and 1970, respectively. Post-doctoral fellow in crystallography at the State University of New York in Stony Brook from 1970 to 1971. Assistant Professor of Crystallography and Mineralogy at Princeton University from 1971 to 1973. Has been at Stanford University since 1973 where he is Professor and currently Chairman of the Department of Geology and Co-Director of the Stanford Center for Materials Research. Was Visiting Professor in the Chemistry Department, Brookhaven National Laboratory in 1972, in the High Temperature Chemistry and Ceramics Division, Sandia National Laboratory, Albuquerque, New Mexico, in 1983, and in the Laboratoire de Mineralogie-Cristallographie, Universités Paris 6 et 7, in 1984. – Research fields: X-ray and neutron scattering studies of crystalline and amorphous oxides, spectroscopic studies of earth materials with emphasis on understanding structure-property relationships of silicate glasses and melts, applications of synchrotron radiation to geochemical and mineralogical problems, structure and properties of oxide and sulfide surfaces, sorption reactions at solid-water interfaces.

George A. Parks: Born 1931 in Oakland, California. Studied extractive metallurgy at the University of California in Berkeley, receiving the B.S. and M.S. degrees in 1953 and 1954, respectively. Studied extractive metallurgy, surface chemistry, and thermodynamics at the Massachusetts Institute of Technology, receiving the Ph.D. degree in 1959. Joined Stanford University faculty in 1959, where he is Donald and Donald M. Steele Professor of Earth Sciences, Professor of Geology, Professor of Civil Engineering, and currently Associate Chairman of the Department of Applied Earth Sciences. Was visiting scientist at the Swiss Federal Institute for Water Resources and Water Pollution Control (EAWAG) in 1976. – Research fields: surface chemistry and low-temperature thermodynamics of minerals in aqueous systems with emphasis on characterization of mineral surfaces and partitioning reactions.

Catherine J. Chisholm-Brause: Born 1959 in Rochester, Minnesota, USA. Studied geosciences at Harvard University, receiving the A.B. degree in 1981. Was employed by the Cities Service Company, as Geologist, from 1981 to 1983. Received the M.S. degree at Stanford University in 1988 and is currently a candidate for the Ph.D. degree at Stanford, studying low-temperature aqueous and surface geochemistry. – Research interests: surface analytical methods and X-ray absorption spectroscopy in the characterization of reactions between minerals and aqueous solutions.

alternative types of surface accumulation of sorbed ions.

The term *sorption* is used when the exact mechanism of accumulation or attachment of a surface complex is not known; the

* Correspondence: Prof. Dr. G. E. Brown, Jr. Aqueous and Surface Geochemistry Group School of Earth Sciences, Stanford University Stanford, CA 94305-2115 (USA)

process may be true *adsorption*, *absorption*, or precipitation on the adsorbent surface. Much of the past work on sorption processes is based on classical solution chemistry methods and is discussed and referenced in recent overviews by *Stumm* [4], *Davis* and *Hayes* [5], and *Sposito* [2]. A distinction is made between *outer-sphere* adsorption complexes, in which the adsorbing ion remains hydrated, and *inner-sphere* complexes, in which it loses at least one water of hydration and bonds directly to the solid surface. Sorption of hydrolyzable cations is typically weak at low pH and increases rapidly at a threshold pH, pH_{ads} [6,7]. Sorption of anions is typically weak at high pH, but increases rapidly at a similar pH_{ads} and is strong at low pH [8-10]. This general behaviour has been described in detail by *Schindler* and *Stumm* [11], *Parks* [12], and *Benjamin* and *Leckie* [13] and is illustrated (Fig. 1) by the sorption of $\text{Pb}^{2\oplus}$, $\text{SeO}_3^{2\ominus}$, and $\text{SeO}_4^{2\ominus}$ on α -FeOOH. Cations may precipitate as hydroxides or oxides at high pH, often not far above pH_{ads} . Precipitation may mimic true adsorption if the precipitate is nucleated on the surface of the host solid. Some investigators have suggested that the solubility product governing precipitation may be perturbed near surfaces, allowing precipitation under conditions apparently undersaturated by normal thermodynamic criteria [5,14]. Others have suggested that material dissolved from the host solid may re-sorb simultaneously with sorption of a foreign solute, yielding mixed precipitates or a solid solution on the surface [15]. *Davis* et al. [16] suggested that $\text{Cd}^{2\oplus}$ sorbing onto calcite (CaCO_3) diffuses into a hydrated surface layer, forming a Ca-Cd carbonate hydrate solid solution. These interpretations are supported only indirectly; they have rarely been tested by direct observation at the molecular level.

Sposito [17] and *Motschi* [18] discussed various means of characterizing surface complexes and of distinguishing among *adsorption*, *absorption*, and surface precipitation. They concluded that classical solution chemical approaches are inadequate unless complemented by spectroscopic methods capable of providing more direct structural information. XPS, EPR, and ENDOR spectroscopies have proven valuable for this purpose, and some useful information also has come from vibrational spectroscopy. The types of structural information provided by these methods for sorption complexes are illustrated by several representative studies.

McBride and co-workers [19-26] used a combination of common solution chemical methods and in-situ EPR spectroscopy at room temperature in a series of investigations characterizing sorption complexes of $\text{Cu}^{2\oplus}$, $\text{Co}^{2\oplus}$, $\text{Mn}^{2\oplus}$, and $\text{VO}^{2\oplus}$ on several aluminium oxides and clays. They inferred oxidation state, coordination number, hydrolysis, and orientation of the sorbing ion. In addition, they attempted to detect multiple sorption sites and to distinguish

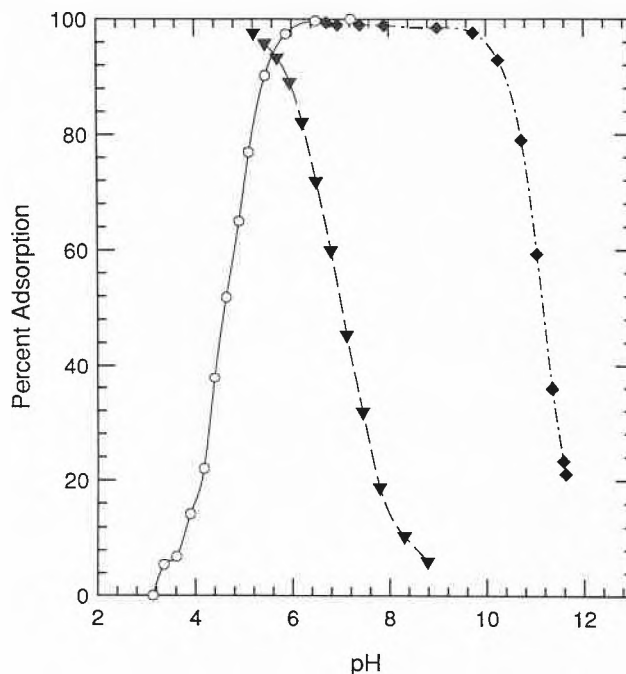


Fig. 1. Metal ion uptake on α -FeOOH (goethite) as a function of pH for initial solutions of 0.002 M $\text{Pb}^{2\oplus}$ (\circ), 0.0001 M $\text{SeO}_3^{2\ominus}$ (\blacktriangledown), and 0.0001 M $\text{SeO}_4^{2\ominus}$ (\blacklozenge). Ionic strength for these experiments was 0.1 M with a solid/solution ratio of 30 g/L. Sorption of cations such as $\text{Pb}^{2\oplus}$ increases with increasing pH at the "adsorption edge", which is consistent with more negative surface charge of amphoteric solids with increasing pH. Conversely, sorption for anions increases with decreasing pH, which is consistent with less negative surface charge with decreasing pH. These data are from Ref. [58].

among mono-nuclear, multi-nuclear (i.e., containing more than one sorbate ion), and precipitated species. Similar in-situ studies of $\text{Cu}^{2\oplus}$ sorbed on hydrous δ - Al_2O_3 have been performed by *Motschi* and co-workers [27,28] using EPR and ENDOR spectroscopies. The EPR results are consistent with a pseudo-square planar coordination geometry for the adsorbed copper ion, and the ENDOR results indicate the presence of protons of both axially and equatorially coordinated water bonded to the adion. Estimates of the Cu-H and Cu-O(H_2O) distances were made from proton hyperfine couplings using the dipolar approximation. *Ichikawa* et al. [29] obtained similar information using electron spin echo spectroscopy on $\text{Cu}^{2\oplus}$ sorbed on silica.

Dillard and co-workers used a combination of solution chemistry, electrokinetic measurements, XPS, and SIMS in an extensive series of sorption studies of transition metal ions onto metal oxides, oxide-hydroxides, and clays [30-33]. They found evidence suggesting that Co^{II} sorbed on α -FeOOH is covalently bonded, thus presumably is sorbed as an inner-sphere complex at low pH. At higher pH (7-7.5) they concluded that «surface induced precipitation of $\text{Co}(\text{OH})_2$ occurred on the goethite surface». They also found that cobalt is partially oxidized when sorbed on α -FeOOH and manganese oxides.

Tejedor-Tejedor and *Anderson* [34] used in-situ attenuated total reflection FTIR spectrophotometry to show that phos-

phate adsorbs onto α -FeOOH by ligand exchange, replacing surface hydroxide groups to form an inner-sphere sorption complex. *Sposito* et al. [35] interpreted changes in structural hydroxide bending modes observed in IR and near-IR spectra as evidence that exchangeable Na^{\oplus} in a montmorillonite «loses solvation water and settles into the ditrigonal cavities on the clay surface» as water is removed from the clay by drying.

Most of the common spectroscopic methods employed in the study of sorption complexes have certain weaknesses. Both EPR and ENDOR methods are restricted to paramagnetic ions. EPR results rely on qualitative comparison of spectra from sorption samples and model compounds, thus provide indirect measures of coordination number and interatomic distances, and only inferential discrimination among *adsorption*, *absorption*, and precipitation. ENDOR spectroscopy can provide more direct structural information, but is commonly used at temperatures so low (10-20 K) that results for the frozen solution may not be applicable at room temperature. XPS methods are useful for compositional and oxidation state analyses of sorbates, but, since samples must be dried and examined in a high-vacuum environment, the structures and compositions of surface complexes and precipitates may be altered. Vibrational spectroscopy methods can be used for in-situ, room temperature studies of sorption but are neither element specific nor easily quantified.

X-ray absorption spectroscopic methods (EXAFS and XANES) employing high-intensity X-ray sources eliminate some of these weaknesses. Like EPR, ENDOR, and XPS, X-ray absorption spectroscopy (XAS) is element specific and sensitive to low element concentrations (equivalent to > 0.1 mM); however it is applicable to a much wider range of sorbing elements and sorbents than the magnetic resonance methods. XAS, unlike XPS, does not require drying of samples or vacuum conditions and can be used at room temperature. Most importantly, XAS can provide direct measures of average interatomic distances between the sorbed ion and its first and second neighbors and average coordination number and atomic identities in each of these shells. This information can be used to discriminate among various types of sorption complexes at solid/water interfaces.

2. X-Ray Adsorption Spectroscopy

A number of detailed discussions of synchrotron-based X-ray absorption spectroscopy (XAS) are available in the literature^[36-40]. The XAS methods known as EXAFS (Extended X-ray Absorption Fine Structure) spectroscopy and XANES (X-ray Absorption Near Edge Structure) spectroscopy are particularly valuable for structural characterization of surface complexes because of the following features:

- (1) EXAFS and XANES spectroscopies are element specific, bulk methods, giving information about the local average structural environment of the absorbing atom. They can be used to study compositionally complex materials.
- (2) Synchrotron-based XAS can be used to study most elements in different states of matter (solid, liquid, gas) at concentration levels of ppm to high weight percentages.
- (3) XAS is a local structural probe which «sees» only the two or three closest shells of neighbors around an absorbing atom ($\leq 5-7$ Å).
- (4) The time required for photon absorption is $\approx 10^{-16}$ seconds, compared to $\approx 10^{-12}$ seconds for interatomic vibrations. Thus EXAFS spectroscopy averages over all local distances around an absorbing atom.
- (5) For many systems, EXAFS analysis is capable of yielding average distances accurate to ± 0.02 Å and average coordination numbers to $\pm 20\%$, assuming that systematic errors have been minimized in the experiment and data analysis and that static and thermal disorder is small.
- (6) Although presently qualitative relative to EXAFS analysis, XANES spectroscopy can provide complementary information about the oxidation state of the sorbed atom and the symmetry and bonding of its local environment. By comparison of the XANES spectra of unknown and model

compounds, the similarity of an atom's local environment in the two compounds can be tested.

The steps in EXAFS data analysis necessary to extract accurate interatomic distances, number, and identities of first- and second-neighbor shells around an absorber are presented briefly as part of the discussion of Co sorption on γ -Al₂O₃ and TiO₂ (rutile) below. A more extensive discussion of the theory and analysis of EXAFS spectra, with particular reference to the characterization of sorbed aqueous metal complexes, is presented elsewhere^[41].

3. Experimental Strategy and Procedure

Fluorescence-yield EXAFS spectroscopy is one of the few methods capable of providing direct structural information on dilute species sorbed on wet surfaces at room temperature^[40,42]. Fluorescence X-ray emission arises from de-excitation of the 1s core hole generated by absorption of an incident X-ray photon. Fluorescent yield, I_f , is directly proportional to the number of absorption events for dilute samples, and I_f/I_0 is proportional to μ , the absorption coefficient of the sample. This method minimizes matrix absorption effects and makes use of large solid angle detection to maximize signal-to-noise ratio (S/N); it permits the use of filters to selectively absorb unwanted fluorescence as well as Compton and elastic scattering from the sample, which also enhances S/N. Key requirements for these measurements are (1) sufficient sorbate concentration to produce measurable X-ray fluorescence, (2) very low concentration of the element of interest in the bulk oxide or solution phase to maximize the contribution of the surface species to the total fluorescence signal, (3) an X-ray excitation energy high enough to minimize the effects of matrix and water absorption of the fluorescent X-rays, and (4) sufficient differences between the backscattering amplitudes and phases of the sorbing element (A) and elements in the adsorbent (B) to permit discrimination between A and B among second neighbors. This last requirement is needed to permit discrimination between mono-nuclear and multi-nuclear sorption species, if present. This requirement constrains the types of sorption systems that can be studied by EXAFS spectroscopy. For example, it precludes study of Co sorbed on iron oxides due to the similarity of backscattering amplitudes and phase shifts for Co and Fe, which would make these atoms indistinguishable by EXAFS. High surface area solids must be used to provide detectable concentrations of the sorbing element, currently the atomic equivalent of ≥ 0.1 millimolar in the excited sample volume.

3.1. Sample Preparation

In general, sorption samples were prepared by equilibrating the sorbent with appropriate solutions containing the sorbate element at concentrations and pH values selected to avoid precipitation and to achieve maximum uptake from solution consistent with a desired surface coverage. The surface coverages and metal uptake achieved for each system studied are listed in Table 1. After equilibration for a minimum of 16 hours, the samples were centrifuged to remove as much liquid as possible, typically between 80 and 90%. The remaining wet suspensions or pastes were mounted in Teflon cells with thin Mylar windows. In some cases, a portion of the removed supernatant was saved for later EXAFS spectroscopic examination to verify that the remaining sorbate concentration was low. When at low concentration, the remaining solute in the wet sample should make no significant contribution to the EXAFS spectra from sorbed species.

3.2. Data Collection and Analysis

All EXAFS data were collected at the Stanford Synchrotron Radiation Laboratory (SSRL) on wiggler-magnet beam lines during dedicated running conditions (3.0 GeV and 40–90 mA beam current). In each experiment, fluorescence-yield data were collected using a Stern-Heald type detector^[43]. These experiments would not have been possible without the use of wiggler beam lines, dedicated running conditions, and fluorescent-yield detection because of the low element concentrations in our samples and the consequent need for very high incident beam intensities and high efficiency detectors. EXAFS data were analyzed in the manner described below and were fit using Fourier-transform least-squares fitting methods and the plane-wave formalism^[36,37]. EXAFS spectra were also collected from aqueous solutions of appropriate salts to provide model spectra representative of the simple metal aqua complex. The crystalline model compounds used for the system selenium on α -FeOOH were MgSeO₃·6H₂O, (NH₄)₂SeO₄, and [Co(NH₃)₅OSeO₂](ClO₄)·H₂O; the model compound for the systems cobalt on γ -Al₂O₃ and on TiO₂ (rutile) was Co(OH)₂; those for the system lead on γ -Al₂O₃ were PbO(orthorhombic) and β -Pb₆O(OH)₆(ClO₄)₄·H₂O.

4. Results and Discussion

4.1. Cobalt on γ -Al₂O₃ and TiO₂

The sorption of Co²⁺ at the Al₂O₃/water and TiO₂(rutile)/water interfaces has been studied using conventional surface chemistry methods^[44,45], XPS^[46,47], and most recently by our group using XAS^[48]. James and Healy^[44] were able to simulate extensive sorption density data with a model

that assumes sorbed $\text{Co}^{2\oplus}$ retains its inner hydration shell. They observed an unusually rapid increase in sorption density with pH when the solution phase approached saturation with respect to $\text{Co}(\text{OH})_2$ and suggested surface-induced precipitation as a possible explanation. *Tewari* and co-workers^[46,47] interpreted similarity in the Co 2p_{3/2} binding energies of $\text{Co}(\text{OH})_2$ and Co^{II} sorbed at high surface coverage on Al_2O_3 at 30 °C as evidence for surface-induced precipitation of $\text{Co}(\text{OH})_2$ in agreement with *James* and *Healy*. This interpretation of the XPS data has been challenged^[49] with the argument that the effect of Co spin states must be accounted for before the spectral similarity between a model compound and an unknown can be used to identify the unknown.

In our XAS work, comparison of Co K-edge XANES spectra for $\text{Co}^{2\oplus}$ on $\gamma\text{-Al}_2\text{O}_3$, $\text{Co}^{2\oplus}$ on TiO_2 , crystalline $\text{Co}(\text{OH})_2$, and aqueous $\text{Co}(\text{NO}_3)_2$ solution (Fig. 2) shows that the local environments of $\text{Co}^{2\oplus}$ sorbed on $\gamma\text{-Al}_2\text{O}_3$ and TiO_2 are significantly different from each other, indicating different local environments for $\text{Co}^{2\oplus}$ on the two surfaces. Furthermore, the spectra for these sorption samples are different from that of $\text{Co}(\text{OH})_2$ and the aqua complex of $\text{Co}^{2\oplus}$ in the solution. This observation suggests that Co in our sorption samples has a local structural environment distinctly different from that in $\text{Co}(\text{OH})_2$. If crystalline $\text{Co}(\text{OH})_2$ is a reasonable structural model for a surface precipitate of Co hydroxide, then surface precipitation can be ruled out as the mode of accumulation for $\text{Co}^{2\oplus}$ sorbed on $\gamma\text{-Al}_2\text{O}_3$ or TiO_2 (rutile) under our experimental conditions. The lack of similarity of the XANES spectra for our sorption samples relative to that of $\text{Co}^{2\oplus}(\text{aq})$ is strong evidence that Co does not form an outer-sphere complex at either oxide/water interface. Moreover, the broader main absorption edges for the two sorption samples could be due to a broader distribution of distances around Co relative to the $\text{Co}^{2\oplus}(\text{aq})$ complex, which would be expected to have a shell of six water molecules with a single Co–O distance. Finally, none of these four spectra displays a significant 1s to 3d pre-edge feature, indicating that $\text{Co}^{2\oplus}$ in each of these samples is in a fairly regular, near-centrosymmetric local coordination environment, such as a slightly distorted octahedron.

The background-subtracted EXAFS data for (a) solid $\text{Co}(\text{OH})_2$, (b) $\text{Co}^{2\oplus}$ on $\gamma\text{-Al}_2\text{O}_3$, (c) $\text{Co}^{2\oplus}$ on TiO_2 , and (d) 12 mM $\text{Co}(\text{NO}_3)_2$ solution are shown in Fig. 3. In order to extract quantitative estimates of the distance, number, and types of nearest neighbors surrounding sorbed Co ions, we must begin data analysis by Fourier transforming the EXAFS functions (Fig. 4). This transformation produces a radial structure function (rsf), which is similar to a radial distribution function but contains only pair correlations involving the absorber. It must be corrected for phase shifts caused by interaction of the outgoing and

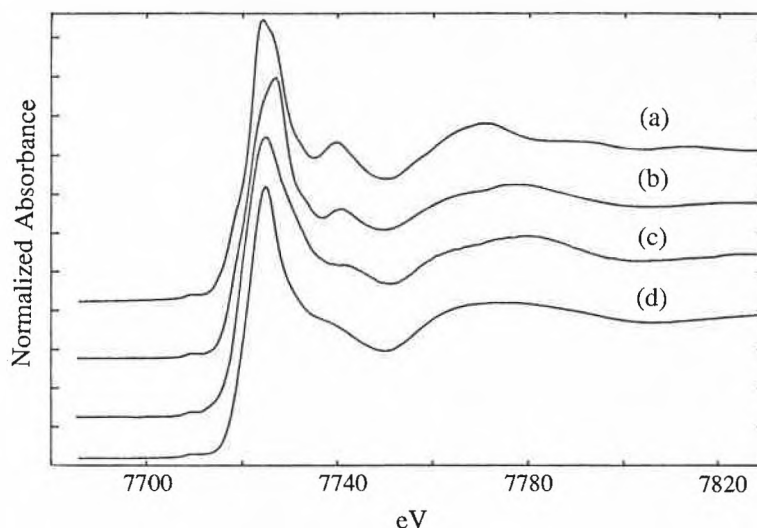


Fig. 2. Co K-XANES spectra for (a) $\text{Co}(\text{OH})_2$, (b) $\text{Co}^{2\oplus}$ sorbed on Al_2O_3 , (c) $\text{Co}^{2\oplus}$ sorbed on TiO_2 , and (d) 12 mM $\text{Co}(\text{NO}_3)_2$ aqueous solution. The marked differences in the edge region (7715–7735 eV) reflect different structural environments for Co in each of these samples. The small amplitude of the pre-edge feature at about 7709 eV is permissive evidence that Co is located in a slightly distorted octahedron for all samples.

backscattered photoelectron waves with the potentials of the atoms^[6]. The real part of the Fourier transform consists of a sum of radial peaks located at R_i , the distance between the absorber and neighboring atomic shells uncorrected for phase shift. The peak areas in the rsf contain information about the number and type of nearest neighbors around the absorber.

The relationships between frequency and distance and among amplitude, coordination number, and atom type must be calibrated before accurate distances, coordination numbers, and atomic identities of atoms around the absorber can be derived for the sorption complex. This step is accomplished either theoretically or by ex-

traction of these relationships from EXAFS spectra of the same element in model compounds. Model compounds must have well-known structures and contain atom pairs and coordination environments similar to those expected in the sorption complexes. The EXAFS data, collected as absorbance versus energy, are first converted to k -space ($|k| = \{2m(E - E_0)\hbar^{-2}\}^{1/2}$), where m is the reduced mass of the electron, \hbar is Planck constant, E is the energy of the incident X-ray beam, and E_0 is the threshold energy of the atom, which in theory is the energy above which the electron is no longer bound to its parent atom. The data are then Fourier transformed and each major peak in the transform is back-

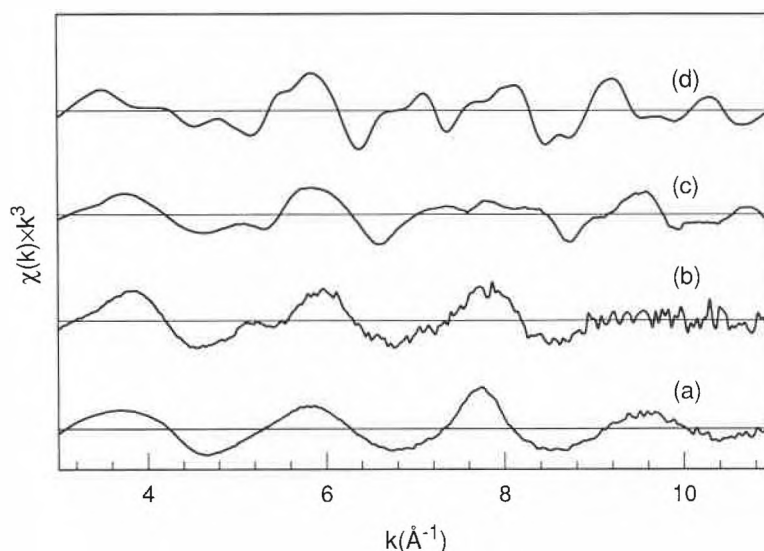


Fig. 3. Background-subtracted, k^3 -weighted EXAFS functions for (a) $\text{Co}(\text{OH})_2$, (b) $\text{Co}^{2\oplus}$ sorbed on Al_2O_3 , (c) $\text{Co}^{2\oplus}$ sorbed on TiO_2 , and (d) 12 mM $\text{Co}(\text{NO}_3)_2$ aqueous solution. These data are Fourier transformed to yield radial structure functions (shown in Fig. 4), which are analyzed to determine bond distances and coordination numbers.

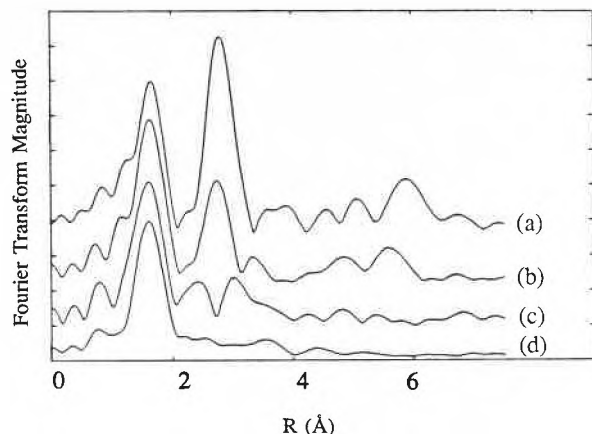


Fig. 4. Radial structure functions (rsf's) for (a) $\text{Co}(\text{OH})_2$, (b) $\text{Co}^{2\oplus}$ sorbed on Al_2O_3 , (c) $\text{Co}^{2\oplus}$ sorbed on TiO_2 , and (d) 12 mM $\text{Co}(\text{NO}_3)_2$ aqueous solution. The first peak is attributed to first-neighbor oxygen atoms, and its amplitude reflects the number of first-shell oxygens surrounding Co. The second peak in (a), (b), and (c) is due to second-shell atoms surrounding Co. Note the lower amplitude of this peak in (b) and (c) relative to (a) and the absence of this peak in (d). A peak at about 6 Å due to fourth-shell Co atoms is present in (a) and, with lower amplitude, in (b). The fourth-shell peak is absent in (c) and (d).

transformed separately to yield contributions to the total EXAFS function expected from individual shells of neighbors. The background-subtracted EXAFS function can be related to distance, number, and disorder of each shell of neighbors surrounding the absorber and to functions describing the k-dependence of backscattering amplitude and phase shift using an appropriate theoretical EXAFS equation^[36,37]. The amplitude and phase-shift functions are estimated by least-squares fitting of this equation to the back-transformed EXAFS function of the model compound, after fixing the distances, coordination numbers, and disorder parameters at the known values of the model compound. EXAFS spectra from sorption samples are analyzed in similar fashion, except that backscattering amplitude and phase-shift functions are fixed at values refined from the model compound, and distance, coordination, and disorder parameters are determined by fitting.

When appropriate model compounds are not available, theoretical estimates of phase-shift and backscattering amplitude functions may be used^[50], though at the possible cost of reduced accuracy. In our work, model compounds were used to provide parameters for the Co–O, Co–Co, Pb–O, and Se–O atom pairs. Parameters for the Se–Co pair were approximated by parameters for the Se–Fe pair, which were derived from model compound data. Theoretical parameters were used for the Co–Al, Co–Ti, Pb–Al, and Pb–Pb atom pairs. The identities of atoms in the first and second shells around an absorber are determined by repeating the fitting process for various possible combinations of backscattering atoms. The atomic identities that yield the best fit are assumed correct. This procedure is possi-

ble because of the significant differences in backscattering amplitudes and phase shifts of different atom pairs^[50].

Least-squares fitting of the back-transforms of the first peak in the radial structure function (rsf) from the Co sorption data yielded six nearest-neighbor oxygens at 2.08 Å for each case. Fitting the second major peak in the rsf of (b) (Fig. 5a, b) resulted in four Co atoms at 3.12 Å and about one Al at 3.20 Å. A third major peak in the rsf at about 5.7 Å was fit to about one Co at 6.1 Å. These Co–Co distances are 0.05 to 0.25 Å shorter and the number of second-neighbor Co atoms are smaller than those in $\text{Co}(\text{OH})_2$. We infer that the one Co neighbor at 6.1 Å in (b) is co-linear with the Co(1)–Co(2) bond, by analogy with the strong Co feature at 6.35 Å in $\text{Co}(\text{OH})_2$. In the latter compound, the 6 fourth-neighbor Co atoms are co-linear with the Co(1)–Co(2) bond, whereas the 18 third-neighbor Co atoms are not and do not contribute significant amplitude to the $\text{Co}(\text{OH})_2$ rsf in the 5.5 Å region. For $\text{Co}^{2\oplus}$ on TiO_2 , fitting the second feature in the rsf centered at ≈ 3 Å resulted in 1.4 Co atoms at 3.36 Å and about one Ti atom at 3.31 Å (Fig. 5c, d). Unlike samples (a) or (b), no strong fourth-shell Co peak is present in

the case of sorption sample (c).

Inclusion of metal ions of the oxide (Al or Ti) in the second shell around the sorbed Co, together with second-neighbor Co, produced significantly better fits than only second-neighbor Co atoms (Fig. 5b, d). This observation leads to the conclusion that Co is bonded directly to the oxide surface in cases (b) and (c). The presence of second-neighbor Co around the sorbed Co indicates the presence of multi-nuclear sorption complexes. To the best of our knowledge, this is the first direct structural evidence for multi-nuclear metal sorption complexes on oxide surfaces^[51]. Comparison of the radial structure functions (rsf) and the fits from the two sorption samples (b and c) with that of solid $\text{Co}(\text{OH})_2$ suggests that Co is present as a true adsorption complex and not as a precipitate. Furthermore, comparison of the rsf's and fits of (b) and (c) with that of the hexaaqua Co^{II} in the nitrate solution (d) indicates that the sorption complex is the inner-sphere type because of the presence and absence, respectively, of second-neighbor Al atoms in the sorption sample and aqueous $\text{Co}^{2\oplus}$ solution. The small number of Al or Ti nearest neighbors in the sorption complexes (b or c) is strong evidence against significant diffusion (absorption) of Co into the oxides.

Several observations suggest that the properties of the solid/water interface influence the adsorption complex. For example, $\text{Co}^{2\oplus}$ adsorbs more strongly and in a different pH range on TiO_2 (rutile) than on $\alpha\text{-SiO}_2$ ^[44]. In addition, $\text{Ni}^{2\oplus}$ precipitates as an amorphous «active» hydroxide in the presence of $\alpha\text{-SiO}_2$ surfaces whereas in the presence of $\alpha\text{-Al}_2\text{O}_3$, it nucleates as more ordered «inactive» $\text{Ni}(\text{OH})_2$ ^[52]. In our study, the large number of second-neighbor Co atoms in the sorption complexes of $\text{Co}^{2\oplus}$ on $\gamma\text{-Al}_2\text{O}_3$ indicates a multi-nuclear complex containing an average of 6 cobalt atoms. In contrast, the small number of second-neighbor Co atoms in the sorption complex of $\text{Co}^{2\oplus}$ on TiO_2 indicates a much smaller species, containing an average of only 2–3 cobalt atoms. The surface coverages were roughly the same in both cases (Table 1).

In summary, these results support the general idea that the nature of the oxide surface influences the characteristics of the sorption complex formed.

Table 1. Characteristics of Sorption Samples.

Sorbate	Sorbent	$A_s^{(1)}$	$C_i^{(2)}$	pH	Uptake (%)	$\Gamma^{(3)}$
$\text{SeO}_3^{2\ominus}$	$\alpha\text{-FeOOH}$	52	5	2.5	> 90	3.20
$\text{SeO}_4^{2\ominus}$	$\alpha\text{-FeOOH}$	52	2	3.5	> 90	1.22
$\text{Co}^{2\oplus}$	$\gamma\text{-Al}_2\text{O}_3$	117	18	6.8	96	1.23
$\text{Co}^{2\oplus}$	TiO_2	23	1.7	6.7	95	1.29
$\text{Pb}^{2\oplus}$	$\gamma\text{-Al}_2\text{O}_3$	117	15	6.0	> 95	1.22

⁽¹⁾ A_s = specific surface area of the sorbent in m^2/g .

⁽²⁾ C_i = initial sorbate concentration, millimolar.

⁽³⁾ Γ = calculated adsorption density, $\mu\text{mol}/\text{m}^2$.

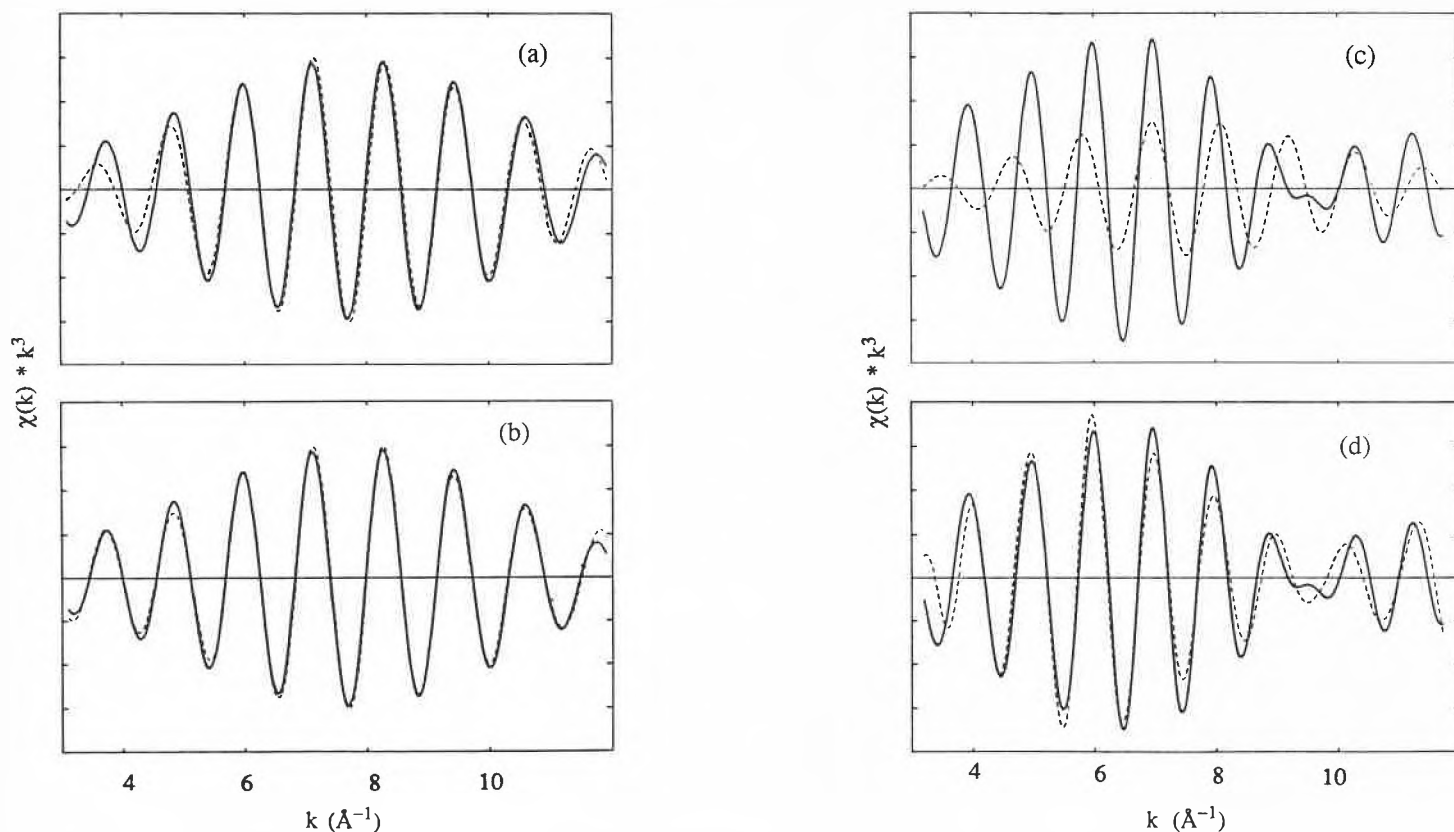


Fig. 5. (a) and (b) are comparisons of the EXAFS function generated by Fourier backtransforming the second radial structure function peak for $\text{Co}^{2\oplus}$ sorbed on Al_2O_3 (solid line) with a least-squares fit theoretical EXAFS function (dashed line) assuming (a) only Co atoms in the second shell and (b) Co and Al atoms in the second shell around the central Co atom. – (c) and (d) are comparisons of the EXAFS function generated by Fourier backtransforming the second rsf peak for $\text{Co}^{2\oplus}$ sorbed on TiO_2 (solid line) with a least-squares fit theoretical EXAFS function (dashed line) assuming (c) only Co atoms and (d) Co and Ti atoms in the second shell around the central Co atom. – For both sorption sample spectra, significantly better fits were achieved by assuming that both Co and metal ions of the oxide (Al or Ti) were present in the second coordination shell.

4.2. Lead on $\gamma\text{-Al}_2\text{O}_3$

The sorption of $\text{Pb}^{2\oplus}$ on $\gamma\text{-Al}_2\text{O}_3$ has been studied by Hohl and Stumm^[53] who found it necessary to assume two types of adsorption complex, one involving a uni-dentate site and the other a bi-dentate site, in order to simulate experimental sorption data with a constant capacitance adsorption model. Davis and Leckie^[54], using an electrical triple-layer adsorption model to interpret the same experimental data, concluded that two uni-dentate type complexes were needed and that the bi-dentate type complex was unnecessary. The figures used by both groups to illustrate the sorption reactions imply inner-sphere complexes. Hayes and Leckie^[55] later emphasized the necessity of distinguishing between inner- and outer-sphere complexes explicitly.

Most recently, our group used XAS^[56, 57] to address these questions. XANES spectra are shown in Fig. 6. The presence of a small shoulder at about 13050 eV in the derivative spectra of the sorption samples at the same energy as a major feature in the Pb model compounds (Fig. 7) suggests the presence of Pb among second-neighbor atoms in the 15 mM sorption sample. This feature is absent in the $\text{Pb}^{2\oplus}(\text{aq})$ sample as it should be. Fourier transforms of the

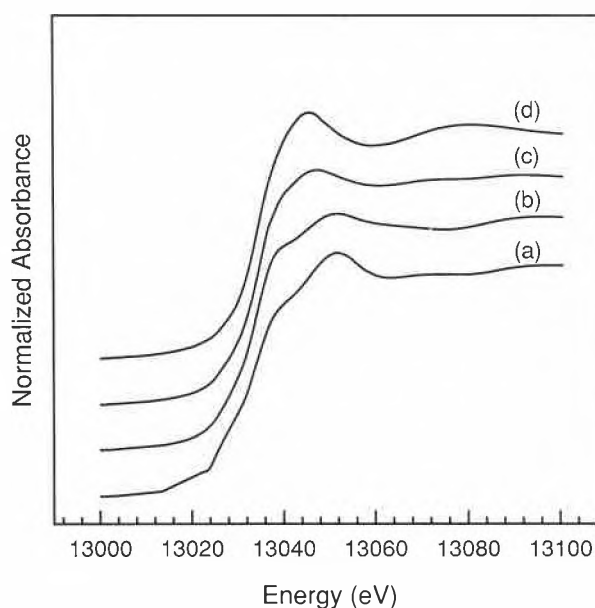


Fig. 6. Pb L_{III} -XANES spectra for (a) PbO (orthorhombic), (b) $\beta\text{-Pb}_6\text{O}(\text{OH})_6(\text{ClO}_4)_4 \cdot \text{H}_2\text{O}$, (c) 15 mM $\text{Pb}^{2\oplus}$ sorbed on Al_2O_3 , and (d) 15 mM $\text{Pb}(\text{NO}_3)_2$ aqueous solution. The presence of two shoulders on the absorption edge for sample (a) reflects the presence of second-shell metal atoms. The marked differences between the spectra for the sorption sample (c) and those of the model compounds (a, b, and d) indicate that the local structural environments of Pb in these samples are different. The presence of two peaks in the region 13060–13100 eV of the spectra for samples (a), (b), and (c) indicates the presence of second-shell metal atom(s).

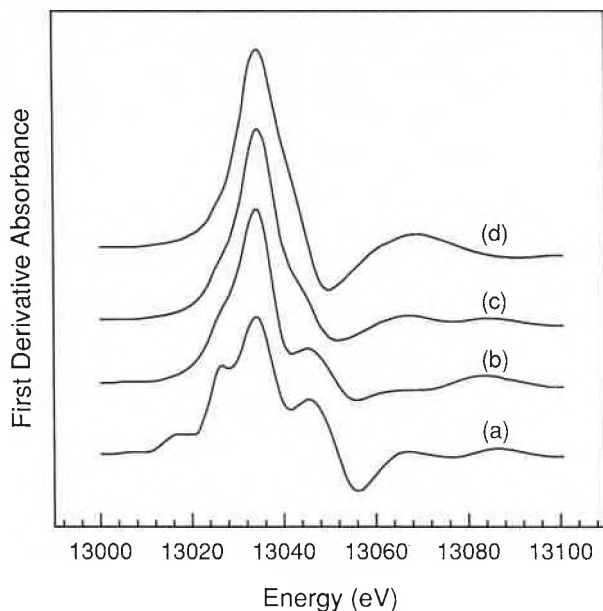


Fig. 7. First derivatives of the Pb L_{III} XANES spectra shown in Fig. 6: (a) PbO (orthorhombic), (b) β - $Pb_6O(OH)_6(ClO_4)_4 \cdot H_2O$, (c) 15 mM $Pb^{2\oplus}$ sorbed on Al_2O_3 , and (d) 15 mM $Pb(NO_3)_2$ aqueous solution. The shoulders in the normalized edge spectra (Fig. 6) due to second-shell metal atoms are indicated by small peaks in the derivative spectra at ≈ 13027 and 13045 eV. The two peaks in the 13060–13100 eV region of the normalized edge spectra for (a), (b), and (c) resulting from the first and second coordination shells around the central Pb absorber atom are clearly visible in the first derivative spectra of (a), (b), and (c).

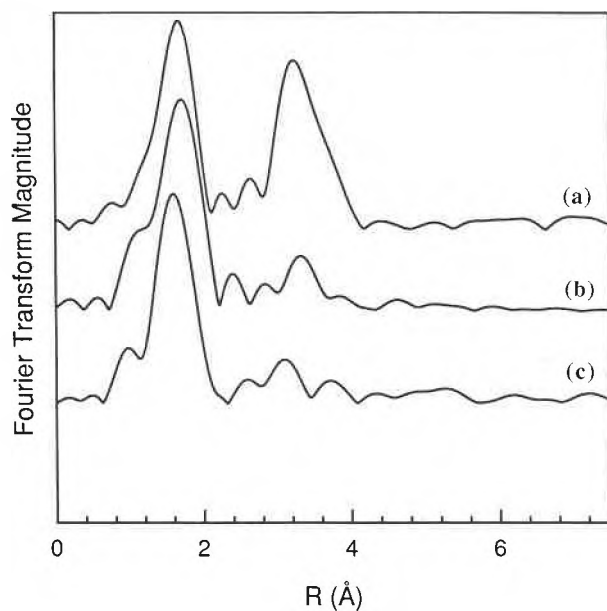


Fig. 8. Radial structure functions for (a) PbO (orthorhombic), (b) β - $Pb_6O(OH)_6(ClO_4)_4 \cdot H_2O$, and (c) 15 mM $Pb^{2\oplus}$ sorbed on Al_2O_3 . A small peak at about 3 Å in (b) indicates the presence of second-shell metal atoms. Fits of backtransform of this peak (Fig. 9) yielded a mixed shell of Pb and Al atoms.

EXAFS functions (Fig. 8) clearly show the presence of a second shell around $Pb^{2\oplus}$ on γ - Al_2O_3 . Fits of the back-transform of the first rsf peak yield one oxygen at 2.23 Å and two oxygens at 2.46 Å. Fits of back-transforms of the second rsf peak (Fig. 9) yield a second-neighbor Pb atom at 3.55 Å and an average of about one Al atom at 3.77 Å, indicating inner-sphere bonding.

The presence of only about one second-neighbor Pb atom indicates either dimeric complexes or a mixture of monomeric and a small fraction of multi-nuclear complexes. This and the presence of an Al in the second-neighbor shell indicate that the sorbed species is not a surface precipitate. The observed Pb–O and Pb–Al distances are consistent with a uni-dentate site in the

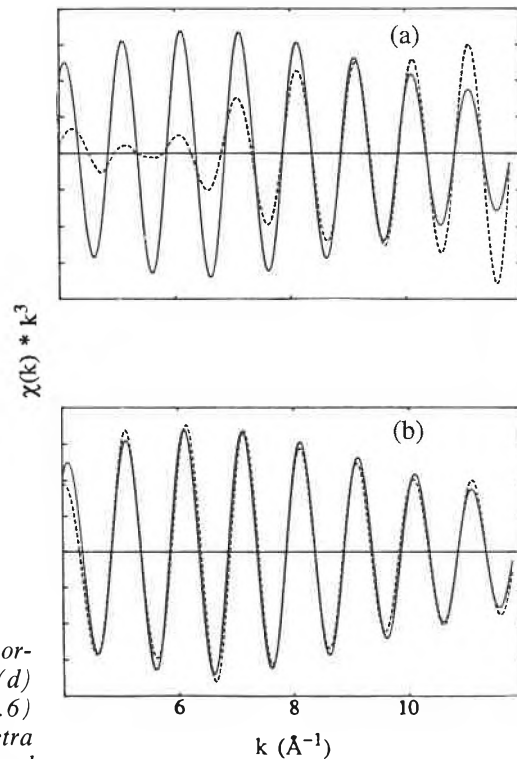


Fig. 9. Comparison of the EXAFS function generated by Fourier back-transforming the second radial structure function peak for 15 mM $Pb^{2\oplus}$ sorbed on Al_2O_3 (solid line) with a least-squares fit theoretical EXAFS function (dashed line) assuming (a) only Pb atoms in the second shell and (b) Pb and Al atoms in the second shell around the central Pb atom.

sense that each Pb in the complex is bonded to a single surface oxygen site; bi-dentate and ter-dentate arrangements have much shorter Pb–Al distances than observed.

In summary, these results provide direct molecular-level evidence that $Pb^{2\oplus}$ forms inner-sphere complexes on γ - Al_2O_3 , probably both uni- and multi-nuclear, involving an average of one surface site per Pb atom.

4.3. Selenium Oxo-Anions on α -FeOOH

Another XAS study of sorption mechanisms focused on selenium oxo-anions on the common ferric iron oxide-hydroxide mineral, goethite (α -FeOOH)^[42]. Fig. 10 illustrates several of the possible geometric arrangements of selenite ions at the goethite/water interface. Conventional surface chemistry studies have shown that selenite is sorbed more strongly than selenate on goethite, suggesting that the two ions are bonded differently^[58]. *In-situ* Se K-edge fluorescence-yield EXAFS spectra of selenate and selenite sorption complexes are shown in Fig. 11. The spectrum of selenate shows a single, damped sinusoidal wave typical of a single shell of four oxygen

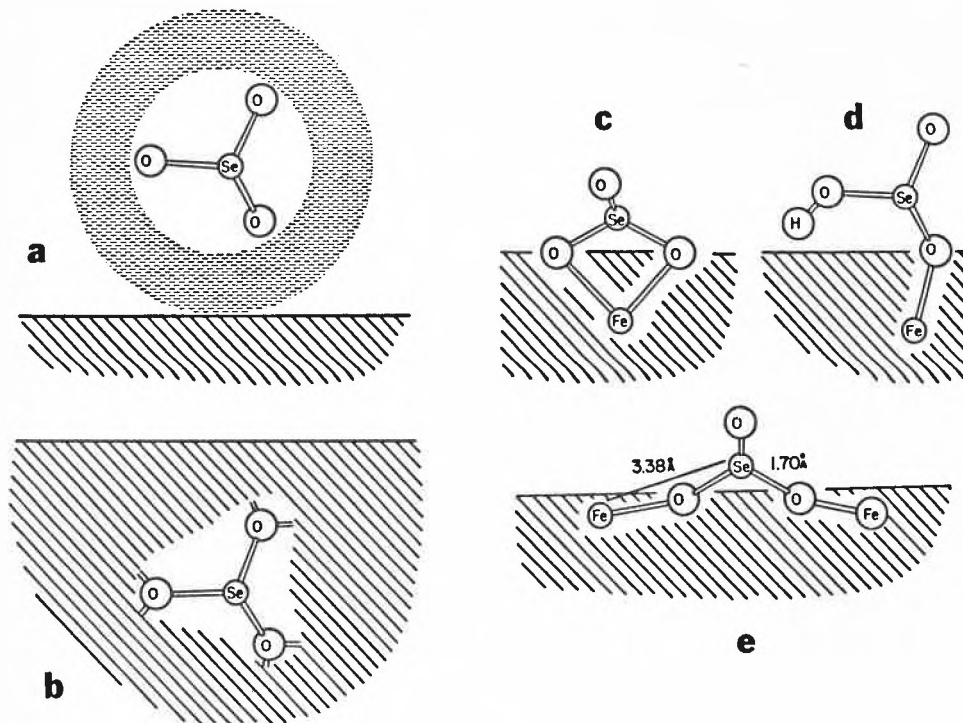


Fig. 10. Schematic drawings of several of the possible geometric arrangements of selenite ions at the α -FeOOH (goethite)/water interface. The solid is indicated by the lined area, and the area above each surface is water. Model (e) is the one most consistent with the fit of the selenite on goethite EXAFS data.

backscatterers, whereas the spectrum of selenite shows a distinctive «beat pattern» characteristic of more than one shell of backscatterers at different distances. Fourier transforms of these spectra (Fig. 12a) show a clear second-shell contribution in the case of selenite but none in the case of selenate. Fitting of the back-transformed spectra using one shell of four oxygens for selenate and two shells for selenite (one shell of three oxygens and one

shell of two irons) gave good fits to the experimental EXAFS data (Fig. 12b). The best-fit models are three oxygens at 1.70 Å and two irons at 3.38 Å around selenium in selenite ions at the goethite/water interface and four oxygens at 1.65 Å around selenium in selenate ions at this interface. These results indicate that selenate is sorbed as an outer-sphere complex and that selenite is sorbed as an inner-sphere complex in a bi-dentate fashion (Fig. 10e).

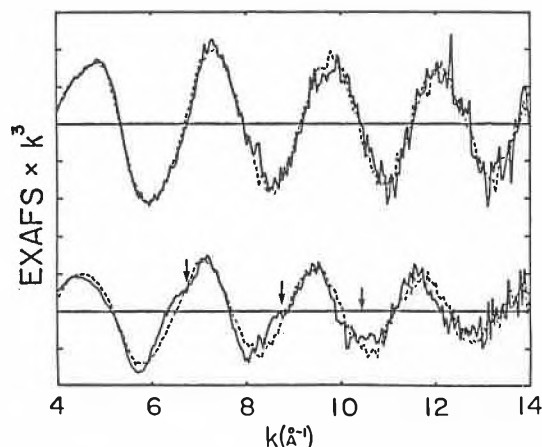


Fig. 11. Background-subtracted, k^3 -weighted Se K-EXAFS spectra for selenate sorbed on goethite (a) and selenite sorbed on goethite (b). Experimental data are shown as solid curves and fits of these data assuming a single shell of four and three oxygen atoms, respectively, for selenate and selenite on goethite are shown as dashed curves. The arrows on spectrum (b) from selenite on goethite indicate features produced by a second shell of metal atoms surrounding Se. Spectrum (a) from selenate on goethite is fit well by a model assuming a single shell of four oxygen atoms around Se.

These structural results provide the first molecular-level explanation for the weak binding of selenate and the strong binding of selenite at the goethite/water interface.

5. Conclusions and Outlook

The distances, number, and identities of first- and second-neighbor atoms around a central atom sorbed on a wet oxide can be determined to a reasonable degree of accuracy by least-squares fitting of Fourier back-transformed peaks in the radial structure functions derived from background-subtracted EXAFS data.

Our study of aqueous Co^{2+} sorbed on γ - Al_2O_3 and TiO_2 (rutile) at about 10% monolayer coverages (pH \approx 6.8) indicates that Co forms inner-sphere complexes. The presence of second-neighbor Co atoms around Co^{2+} sorbed on these wet oxides indicates the presence of multi-nuclear complexes. This is the first direct structural evidence we are aware of for multi-nuclear metal sorption complexes on oxide surfaces. Aqueous Pb^{2+} sorbed on γ - Al_2O_3 at 10% monolayer coverage (pH \approx 6.0) occurs as small (dimeric or a mixture of monomeric and small multi-nuclear), inner-sphere complexes bonded to an average of one surface oxygen site per sorbed Pb atom. These results for sorbed cobalt and lead indicate inner-sphere complexes which are, or include, multi-nuclear species in all cases. On average, each sorbed ion is probably associated with a single surface site.

The observed sizes and local structures of these complexes are influenced by the nature of the solid substrate as well as by the sorbing ion. Inner-sphere complexes are consistent with XPS results suggesting covalent bonding, but the surface precipitation suggested by some XPS work is incompatible with XANES and EXAFS data.

Aqueous selenate (pH 3.5, 5 mM) and selenite (pH 5.6, 2 mM) sorb on α -FeOOH as outer- and inner-sphere complexes, respectively, with selenite bonding to the goethite surface in a bi-dentate fashion. The approximate surface coverages of selenate and selenite were 25% and 10%, respectively.

Finally, the XAS results preclude formation of mixed surface precipitates and diffusion of the sorbate ion into the bulk oxide in all systems studied.

This work demonstrates the utility of synchrotron-based X-ray absorption spectroscopy in providing valuable and, in certain cases, unique structural and compositional information on sorption complexes at solid/water interfaces. Similar applications of fluorescence-yield X-ray absorption spectroscopy to other systems could yield insights into reaction mechanisms in areas such as electrochemistry; colloid chemistry; corrosion of metals, minerals, and building stone; and heterogeneous

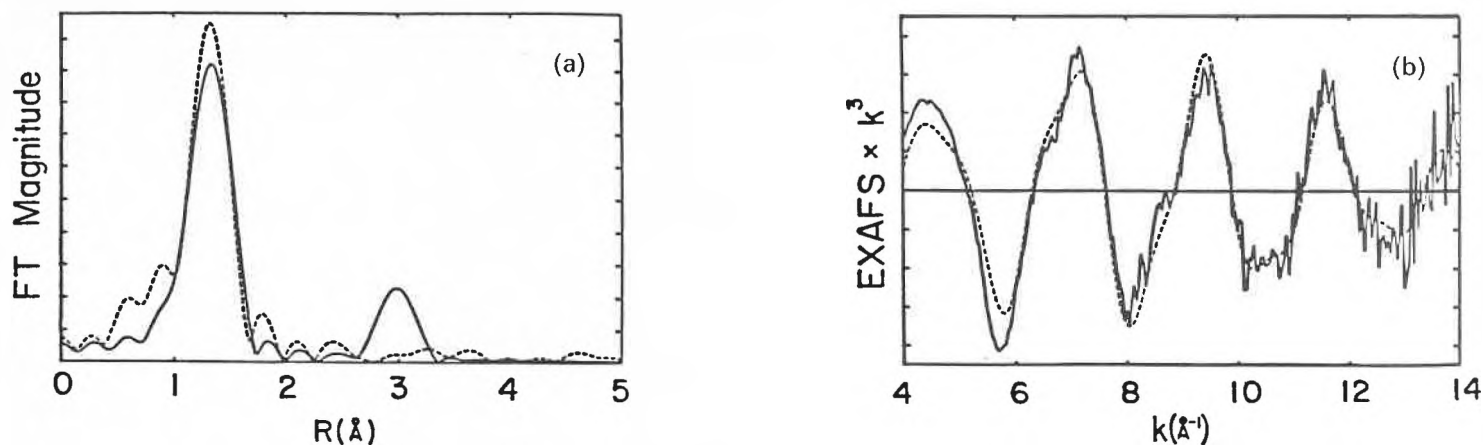


Fig. 12. (a) Radial structure functions for selenite (solid curve) and selenate (dashed curve) sorbed on goethite. (b) Comparison of the EXAFS function generated by Fourier back-transforming the first and second radial structure function peaks for 5 mM selenite sorbed on goethite (solid line) with a least-squares fit theoretical EXAFS function (dashed line) assuming three oxygen atoms at 1.70 Å and two iron atoms at 3.38 Å around selenium.

catalysis. When higher intensity, third generation synchrotron radiation sources are completed in Europe (European Synchrotron Radiation Facility at Grenoble) and the USA (the Advanced Photon Source at Argonne National Laboratory and the Advanced Light Source at Lawrence Berkeley Laboratory) in the mid-1990's, new classes of X-ray absorption spectroscopy experiments will be possible. These include XAS studies of elements at extreme dilution in materials of all types and real time studies of transient phenomena such as photo oxidation-reduction reactions at surfaces.

Acknowledgements: G.E.B. is grateful to Professor Werner Stumm (EAWAG) for providing the opportunity to present these results at a symposium, «Inorganic and Coordination Chemistry: Role of Surfaces», within the Fall Meeting of the Swiss Chemical Society in Berne, October 21, 1988, and to J. O. Leckie for suggesting this opportunity. We thank K.F. Hayes, A.L. Roe, K.O. Hodgson, and J.O. Leckie for fruitful collaborations in the original studies. Garrison Sposito (University of California, Berkeley), Werner Stumm (EAWAG), and Peggy A. O'Day (Stanford University) reviewed the manuscript and provided helpful suggestions. We wish to thank the U.S. National Science Foundation for financial support of this work (Grants EAR-8513488 and EAR-8805440). This work was carried out at the Stanford Synchrotron Radiation Laboratory which is supported by DOE and NIH.

Received: February 1, 1989 [FR 66]

[3] W. Stumm, G. Furrer, B. Kunz, *Croat. Chem. Acta* 58 (1983) 593.
 [4] W. Stumm (Ed.): *Aquatic Surface Chemistry*, Wiley-Interscience, New York (1987).
 [5] J.A. Davis, K.F. Hayes, in J.A. Davis, K.F. Hayes (Ed.): *Geochemical Processes at Mineral Surfaces*, ACS Symp. Ser. 323, American Chemical Society, Washington, DC (1986), p. 2.
 [6] R.O. James, T.W. Healy, *J. Colloid Interface Sci.* 40 (1972) 42.
 [7] W. Stumm, H. Hohl, F. Dalang, *Croat. Chem. Acta* 4 (1976) 491.
 [8] W. Stumm, R. Kummert, L. Sigg, *Croat. Chem. Acta* 53 (1980) 291.
 [9] J.A. Davis, J.O. Leckie, *Environ. Sci. Technol.* 12 (1978) 1309.
 [10] L. Sigg, W. Stumm, *Colloids Surfaces* 2 (1981) 101.
 [11] P.W. Schindler, W. Stumm, in W. Stumm (Ed.): *Aquatic Surface Chemistry*, Wiley-Interscience, New York (1987), p. 83.
 [12] G.A. Parks, in J.P. Riley, G. Skirrow (Ed.): *Marine Geochemistry, 2nd Ed., Vol. 1*, Academic Press, New York (1975), p. 241.
 [13] M.M. Benjamin, J.O. Leckie, *Environ. Sci. Technol.* 15 (1981) 1050.
 [14] H.A. Elliott, C.P. Huang, *J. Colloid Interface Sci.* 70 (1979) 29.
 [15] K.J. Farley, D.A. Dzombak, F.M.M. Morel, *J. Colloid Interface Sci.* 106 (1985) 226.
 [16] J.A. Davis, C.C. Fuller, A.D. Cook, *Geochim. Cosmochim. Acta* 51 (1987) 1477.
 [17] G. Sposito, in J.A. Davis, K.F. Hayes (Ed.): *Geochemical Processes at Mineral Surfaces*, ACS Symp. Ser. 323, American Chemical Society, Washington, DC (1986), p. 217.
 [18] H. Motschi, in W. Stumm (Ed.): *Aquatic Surface Chemistry*, Wiley-Interscience, New York (1987), p. 111.
 [19] M.B. McBride, *Clays Clay Miner.* 24 (1976) 88.
 [20] M.B. McBride, *Clays Clay Miner.* 26 (1978) 101.
 [21] M.B. McBride, *Clays Clay Miner.* 30 (1982) 21.
 [22] M.B. McBride, *Clays Clay Miner.* 30 (1982) 200.
 [23] M.B. McBride, A.R. Fraser, W.J. McHardy, *Clays Clay Miner.* 32 (1984) 12.
 [24] M.B. McBride, in J.A. Davis, K.F. Hayes (Ed.): *Geochemical Processes at Mineral Surfaces*, ACS Symp. Ser. 323, American Chemical Society, Washington, DC (1986), p. 362.
 [25] J.B. Harsh, H.E. Doner, M.B. McBride, *Clays Clay Miner.* 32 (1984) 300.
 [26] C.J. Clark, M.B. McBride, *Clays Clay Miner.* 32 (1984) 407.
 [27] H. Motschi, *Naturwissenschaften* 70 (1983) 519.
 [28] M. Rudin, H. Motschi, *J. Colloid Interface Sci.* 98 (1984) 385.
 [29] T. Ichikawa, H. Yoshido, L. Kevan, *J. Chem. Phys.* 75 (1981) 2485.
 [30] M.H. Koppelman, J.G. Dillard, *J. Colloid Interface Sci.* 62 (1978) 345.
 [31] C.V. Schenk, J.G. Dillard, J.W. Murray, *J. Colloid Interface Sci.* 95 (1983) 398.
 [32] J.G. Dillard, M.H. Koppelman, *J. Colloid Interface Sci.* 87 (1982) 46.
 [33] J.G. Dillard, C.V. Schenk, in J.A. Davis, K.F. Hayes (Ed.): *Geochemical Processes at Mineral Surfaces*, ACS Symp. Ser. 323, American Chemical Society, Washington, DC (1986), p. 503.
 [34] M.I. Tejedor-Tejedor, M.A. Anderson, *Langmuir* 2 (1986) 203.
 [35] G. Sposito, R. Prost, J.-P. Gaultier, *Clays Clay Miner.* 33 (1985) 9.
 [36] B.K. Teo, D.C. Joy (Ed.): *EXAFS Spectroscopy*, Plenum Press, New York (1981).
 [37] T.M. Hayes, J.B. Boyce, *Solid State Phys.* 37 (1982) 173.
 [38] B.K. Teo: *EXAFS: Basic Principles and Data Analysis*, Inorg. Chem. Concepts 9, Springer, Berlin (1986).
 [39] J. Wong, *Mater. Sci. Eng.* 80 (1986) 107.
 [40] G.E. Brown Jr., G. Calas, G.A. Waychunas, J. Petiau, in F. Hawthorne (Ed.): *Spectroscopic Methods in Mineralogy and Geology*, Rev. Mineral. 18 (1988) 431.
 [41] G.E. Brown Jr., G.A. Parks, *Rev. Geophys.* (1989), in press.
 [42] K.F. Hayes, A.L. Roe, G.E. Brown Jr., K.O. Hodgson, J.O. Leckie, G.A. Parks, *Science* 238 (1987) 783.
 [43] F. Lytle, D.R. Sandstrom, E.C. Marques, J. Wong, C.L. Spiro, G.P. Huffman, F.E. Hug-gins, *Nucl. Instrum. Methods* 226 (1984) 542.
 [44] R.O. James, T.W. Healy, *J. Colloid Interface Sci.* 40 (1971) 42.
 [45] P.H. Tewari, A.B. Campbell, W. Lee, *Can. J. Chem.* 50 (1972) 1642.
 [46] P.H. Tewari, N.S. McIntyre, *AIChe Symp. Ser.* 71 (150) (1974) 134.
 [47] P.H. Tewari, W. Lee, *J. Colloid Interface Sci.* 52 (1975) 77.
 [48] C.J. Chisholm-Brause, G.E. Brown Jr., G.A. Parks, *Physica B* 158 (1989) 646.
 [49] D. Briggs, Y.M. Bosworth, *J. Colloid Interface Sci.* 59 (1977) 194.
 [50] B.K. Teo, P.A. Lee, *J. Am. Chem. Soc.* 101 (1979) 2815.
 [51] C.J. Chisholm-Brause, P.A. O'Day, G.E. Brown Jr., G.A. Parks, *Nature (London)*, submitted (1989).
 [52] A. Ahmed, Ph. D. Dissertation, Stanford University (1971).
 [53] H. Hohl, W. Stumm, *J. Colloid Interface Sci.* 55 (1976) 281.
 [54] J.A. Davis, J.O. Leckie, *J. Colloid Interface Sci.* 67 (1978) 3.
 [55] K.F. Hayes, J.O. Leckie, *J. Colloid Interface Sci.* 115 (1987) 564.
 [56] C.J. Chisholm-Brause, A.L. Roe, F.K. Hayes, G.E. Brown Jr., G.A. Parks, J.O. Leckie, *Physica B* 158 (1989) 674.
 [57] C.J. Chisholm-Brause, G.E. Brown Jr., G.A. Parks, *Geochim. Cosmochim. Acta*, submitted (1989).
 [58] K.F. Hayes, Ph. D. Dissertation, Stanford University (1987).

[1] G.A. Parks, *Chem. Aust.* 49 (1982) 389.
 [2] G. Sposito: *The Surface Chemistry of Soils*, Oxford University Press, Oxford (1984); cf. also G. Sposito, *Chimia* 43 (1989) 169.